PLATINUM-SILICIDE SCHOTTKY-BARRIER IR-CCD IMAGE SENSORS*

W. F. Kosonocky, E. S. Kohn, F. V. Shallcross, D. J. Sauer
RCA Laboratories
David Sarnoff Research Center
Princeton, NJ 08540

AND

F. D. Shepherd, L. H. Skolnik, R. W. Taylor, B. R. Capone, S. A. Roosild
Rome Air Development Center
Deputy for Electronic Technology
Hanscom AFB, MA 01731

ABSTRACT

We describe the construction, operation and characteristics of two types of monolithic silicon IR-CCD sensors with platinum-silicide (Pt_xSi) Schottky-barrier detectors. They are a 256-element line sensor and a 25x50-element area sensor. These IR-CCD's can be operated from 50 to 90 K, and are sensitive in the 1.2 to 4.6 μm spectral range. A typical value of the quantum-efficiency coefficient (C_1) of the platinum-silicide detectors is 5%/eV. A photoresponse uniformity of 0.55% rms was demonstrated with the 256-element line sensor. Thermal imaging data are reported for both calibrated infrared sources and human subjects. Noise-equivalent temperatures (NET) of 0.4°C and 1.0°C in 26°C ambient, noise-equivalent powers (NEP) of $8x10^{-12}$ W and $3.36x10^{-11}$ W, and linear dynamic ranges of 5,000 and 1,800 were demonstrated with the line and the area sensors, respectively, for operation with an integration (staring) time of 30 ms. The dynamic range of these infrared sensors, however, can be extended further by operation in a blooming control (saturation) mode.

I. INTRODUCTION

Schottky-barrier infrared detectors offer the possibility for production of highly uniform, monolithic silicon IR-CCD focal plane arrays. Platinum-silicide (Pt_xSi) Schottky barriers on p-type silicon have a barrier height of about 0.27 eV which corresponds to an infrared-response cutoff wavelength of 4.6 μm [1]. Thermal imaging with platinum-silicide IR-CCD arrays was described by Shepherd [1-3], Kohn, et.al. [4], Taylor et.al. [5], Skolnik, et.al. [6], and Capone et.al. [7]. In this paper we will describe the construction, operation, and infrared characteristics of a 256-element line sensor [5,6,8] and a 25x50-element area sensor [7, 9,10]. These devices were designed and fabricated at RCA Laboratories. The reported infrared measurements were made at RADC/ESE.

*The part of this work performed at RCA Laboratories was supported by RADC/ESE and DOD-BISSPO, Hanscom AFB, MA.

II. PLATINUM-SILICIDE SCHOTTKY-BARRIER DETECTORS

The use of Schottky-barrier detectors for infrared imaging has been described extensively in the literature [1-14]. The platinum-silicide (Pt_xSi) detector is formed by depositing a layer of platinum (typically about 600 Å) on a p-type silicon substrate (having resistivity of 10 to 50 Ω-cm) and then sintering it at a temperature in the range of 200 to 650°C. The composition of the Pt_xSi alloy varies with the sintering temperature and time as well as with the initial thickness of the platinum layer [14]. The reaction between the metal and the silicon places the Pt_xSi:Si junction beneath the original surface of silicon, and thus produces diodes free of surface effects and with highly uniform photoresponse. In fact, 1-cm diameter Pt_xSi diodes have been fabricated having rms photoresponse nonuniformities of less than 0.1% [3]. Therefore, the photoresponse uniformity of the platinum-silicide detectors fabricated thus far have

been basically limited by the uniformity of the geometric definition of the detectors. The photoyield, Y, for Schottky emission is given by [2]

$$Y = \frac{C_1 (h\nu - \psi_{ms})^2}{h\nu} \frac{\text{electrons}}{\text{photon}} , \qquad (1)$$

where ψ_{ms} is the barrier height, h Planck's constant, ν the photon frequency and C_1 a factor determined by the geometrical, optical and transport properties of the silicide contact. With $h\nu$ and ψ_{ms} expressed in eV, C_1 is in reciprocal eV. An example of a photoyield curve for a 600 Å Pt/p-Si diode reacted at 320°C is shown in Fig. 1, where we plot $\sqrt{Yh\nu}$ vs $h\nu$. From the graph we find a barrier height of 0.268 eV and a C_1 of 3.6% eV. A

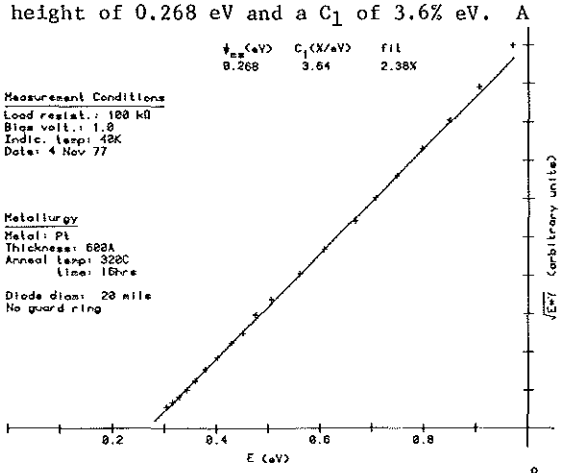

Fig. 1. Photoyield versus energy for 600 Å PtSi diode.

typical value of C_1 for Pt_xSi detectors is 5%/eV. It should be noted, however, that the form of the yield curve (Fig. 1) and the values of C_1 ($3 \leq C_1 \leq 11\%/eV$) are highly dependent on reaction conditions and initial Pt layer thickness. Effects such as electron-phonon mean-free-paths and enhanced thin-film reflections can influence the energy dependence of the photoresponse [12,13]. The effective quantum efficiency for thermal imaging of platinum-silicide Schottky-barrier detectors is rather small, i.e., on the order of 0.1%. However, the demonstrated high uniformity of photoresponse (0.5% rms and better) [3-7] combined with low-noise readout by buried-channel CCD's made the Schottky-barrier IR-CCDs attractive alternatives for many thermal imaging applications. The rather low quantum yield in Schottky detectors can be made up by operating the arrays either in the staring or time-delay-integration mode. Calculations [3] based on present estimates indicate that these devices with 6.25×10^{-5} cm^2 (1 mil^2) detectors should be capable of resolving 0.1°C targets against a 300 K background at standard video frame rates.

III. DEVICE CONSTRUCTION AND OPERATION

A. Technology

The devices were processed using two-level polysilicon buried-channel CCD technology with p^+ channel stops and n^+ diffusions not self-aligned to the polysilicon gates. The substrates used were 20 to 50 Ω-cm, boron-doped, p-type [100] silicon wafers polished on both sides to a final thickness of 10 mils (250 μm). The platinum-silicide detectors were formed by depositing a 500 to 600 Å film of platinum on the Schottky contact holes opened in the oxide (SiO_2) and then sintering at temperatures in the range from 320 to 650°C. After the platinum silicide formation, the remaining platinum was etched off and a 14,000 Å aluminum metalization was deposited and defined to complete the device processing. The platinum-silicide detectors were formed surrounded by implanted n-type guard rings to reduce the excess dark (leakage) current. This was accomplished using the buried-channel implant, typically in the form of phosphorus with a dose of 1 to 2×10^{12} cm^{-2} at 180 KeV.

B. 256-Element IR-CCD Line Sensor

A block diagram of the 256-element IR-CCD line sensor is shown in Fig. 2. A more

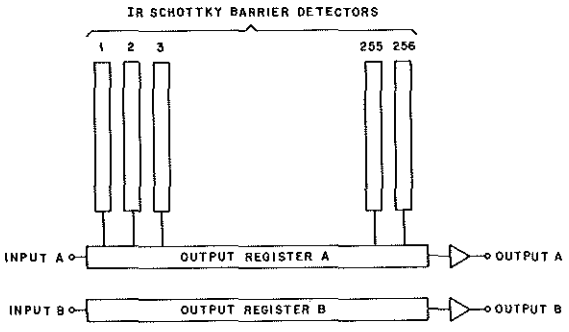

Fig. 2. Block diagram of 256-element IR-CCD line sensor.

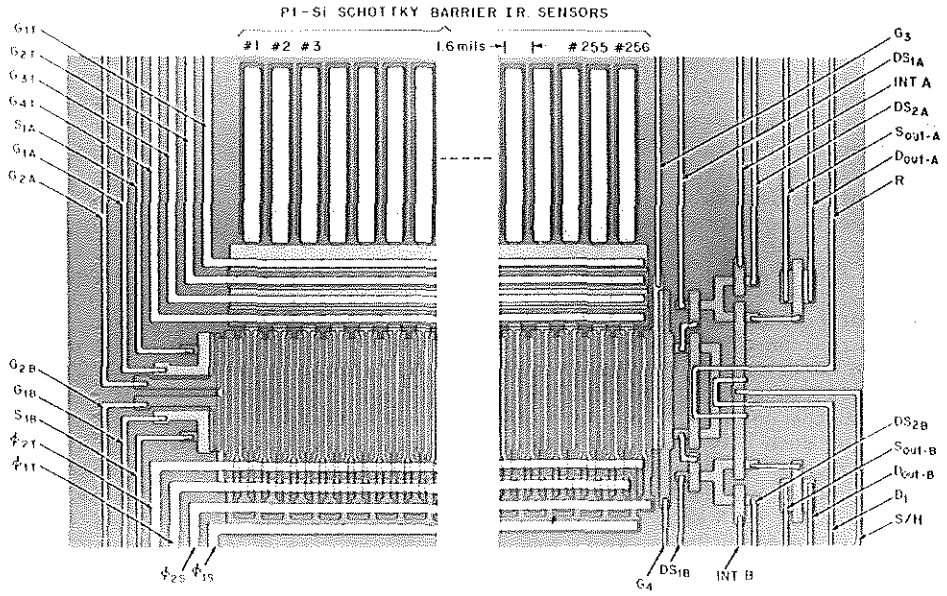

Fig. 3. Photomicrograph of the input and output sections of the 256-element IR-CCD line sensor.

detailed layout of this device is illustrated in Fig. 3, which shows the input and the output sections of the device. The cross-sectional view of the charge-coupling structure between the platinum silicide detectors and the CCD Output Register A is shown in Fig. 4. The platinum-silicide detectors are surrounded by implanted n-type guard rings and are isolated from each other by 5 μm-wide, p^+ channel stops. The effective size of the detectors is 10 μm x 200 μm, and the detectors are spaced on 40 μm centers. The line-sensor chip is 11.3 mm by 1.7 mm.

In addition to a buried-channel CCD, Output Register A, for scanning the infrared detectors, the chip also contains an identical register, Output Register B, driven by the same clock lines. In the tests reported here, the two registers were normally used together to cancel the common-mode clock pick-ups. However, it is also possible with this sensor to perform on-chip frame comparison schemes such as moving-target indication. The output registers are two-level polysilicon, two-phase BCCD's with 40 μm stages, and have been designed rather conservatively with 15 μm gates, 5 μm spaces, and 5 μm gate overlaps.

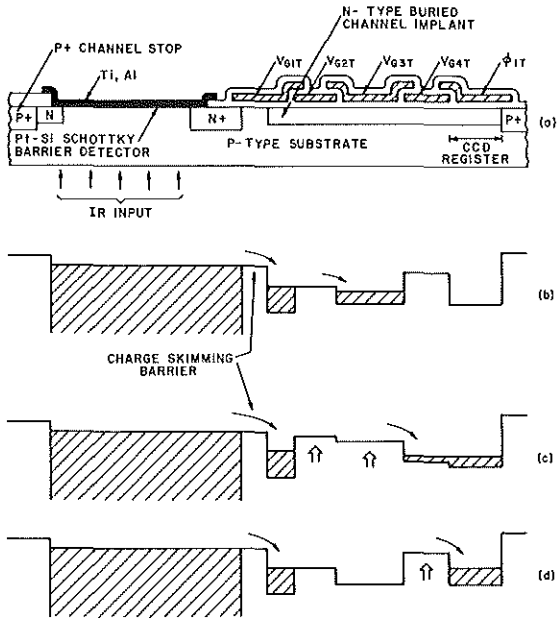

Fig. 4. Construction and operation of the Schottky-barrier detectors operating in the continuous-charge-skimming mode.

The readout of charge from the Schottky-barrier detectors in the line sensor is illustrated in Fig. 4 using the "continuous-charge-skimming" mode*. The detector array is backside illuminated. The function of the surface-channel gate G_{1T} is to maintain a fixed (dc biased) "charge-skimming" barrier that determines the reverse bias voltage for the Schottky diodes. During the integration (stare) time of the optical signal, the detected charge is collected in the charge-integration well under the buried-chanel gate G_{3T} (see Fig. 4(b)). The function of the buried-channel gate G_{4T} is to isolate the charge-integration well from the CCD output register. At the end of the stare time (variable from 10 to 100 ms) the collected charge signal is transferred from the integration well to the serial CCD output register by a form of push clocking (one with slow fall time) as illustrated in Figs. 4(c) and (d). The output-register clock rate can be varied from 1 kHz to 5 MHz. For most of the measurements reported here, stare and line times were maintained at 30 ms and 23 ms, respectively.

Although the line sensor is designed to operate in the continuous-skimming mode, it can also be operated in the more conventional voltage-reset mode illustrated later in Fig. 9 for the area sensor. The continuous-charge-skimming mode minimizes the noise associated with the resetting of the Schottky diodes. Also an interesting property of the continuous-charge-skimming mode is that the Schottky diodes are maintained at a constant potential which can be adjusted to any desired value by controlling the dc voltage V_{G1T}. By maintaining the reverse-bias voltage of the Schottky diodes at a low value, the leakage current and the leakage current spikes (which tend to increase exponentially with voltage) can be maintained at minimum levels. However, if desired, the Schottky diode reverse-bias voltage can be increased to a value at which the leakage current spikes become appreciable. Our tests show that operation with the larger reverse-bias voltage tends to increase the sensitivity of these devices as infrared sensors. Finally it should be added that construction of the line sensor with separate CCD-type, charge-integration wells, results in the charge-handling capacity of the sensor being limited by the design of the CCD readout structure rather than by the normally-smaller depletion-layer capacitance of the Schottky diode.

C. 25x50-Element IR-CCD Area Sensor

A block diagram and a photomicrograph of the area-sensor chip are shown in Figs. 5 and 6. The chip is 5.84 mm square. The area sensor contains 25 columns of detectors with 50 detectors in each. The 25 column, charge-coupled shift registers are interspersed with the detector columns, and connect to a horizontal register at the top of the photo. The output stage is at the top left. The vertical detector spacing is 80 μm, while the horizontal detector spacing is 160 μm. The active area of each detector is 2100 $(\mu m)^2$ or 16.4% of the unit-cell area. The chip is mounted in a 28-pin dual-in-line ceramic package with a 4.75 mm square opening under the chip for near IR illumination. The chip also contains a 62-element line array, not discussed here, and many test devices.

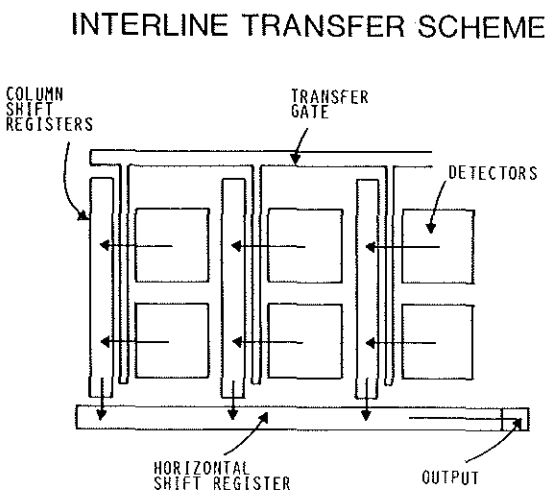

Fig. 5. Block diagram of the 25x50-element IR-CCD area sensor.

*This mode of operation of the CCD imager, developed independently at RCA Laboratories, has been described by [15,16].

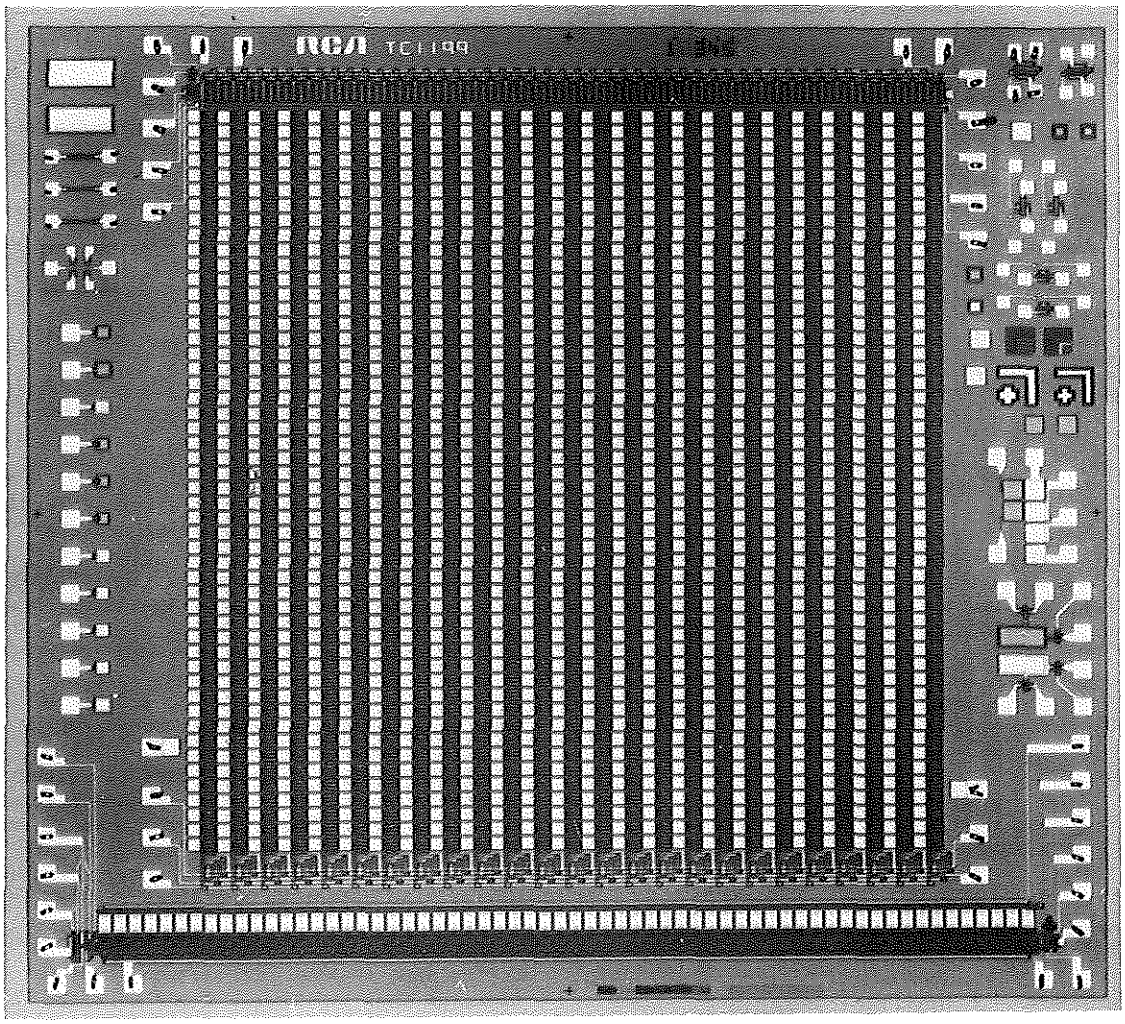

Fig. 6. Photomicrograph of the 25x50-element IR-CCD area sensor.

The construction of the area sensor is illustrated in more detail in the schematic diagram in Fig. 7. This diagram illustrates all of the elements and identifies the electrical terminals. This sensor has an interline-transfer organization. The infrared detectors are separated from the buried-channel CCD (BCCD) column shift register by vertical, surface-channel transfer gates. In the staring mode of operation, the detected image is transferred from the infrared detectors to the BCCD column registers once every frame time. Then, while the detectors integrate a new frame, the original frame is transferred, a line at a time, from the BCCD column registers to the BCCD horizontal output register, from which each horizontal line is read out in series by the floating-diffusion output amplifier. The floating-diffusion sensing-node capacitance of this device is about 0.7 pF, and the voltage gain of the source-follower output circuit is about 0.7. The column registers and output register are two-level-polysilicon, four-phase CCD's with 80 μm-long stages. The vertical column registers are coupled to every second stage of the output register.

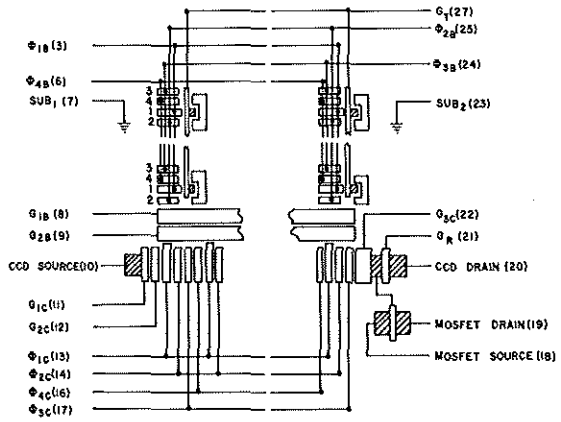

Fig. 7. Schematic diagram of the 25x50-element IR-CCD area sensor.

A detailed description of the platinum-silicide detectors of the area sensor is shown in Fig. 8. This figure illustrates how the effective area of the detector of 2100 $(\mu m)^2$ or 3.36 mil^2 is determined.

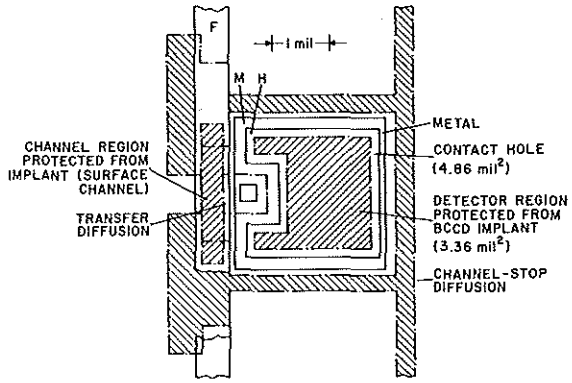

Fig. 8. Scale drawing of the effective detector areas of the 25x50-element IR-CCD area sensor as defined by the Schottky-contact mask and the buried-channel or the guard ring mask.

The area sensor is operated in the voltage-reset mode illustrated in Fig. 9. This

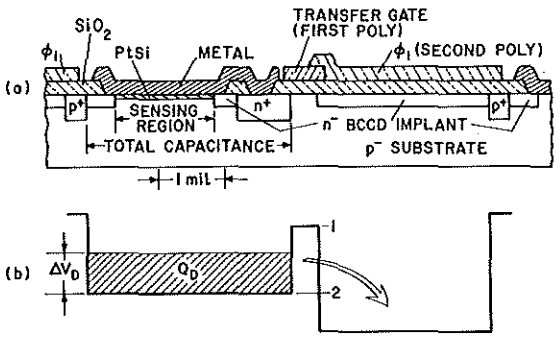

Fig. 9. Construction and operation of area-array detectors: (a) cross section of area sensor showing detector region, transfer structure and shift-register gate. (b) electron-energy profile during voltage-reset operation of detector.

mode was previously referred to as the "vidicon" mode [4,9]. In this mode the (surface-channel) transfer gate is pulsed positively once each frame. The detectors are set to a reverse bias determined by the surface potential under the transfer gate during the transfer pulse. Between transfer pulses, the detectors are discharged by infrared response and by dark current. At each transfer pulse, each detector is set to the same reverse bias as the previous time, so that the charge removed to the CCD well, as in Fig. 9(b), is the true signal from the detector. As in the case of the continuous-charge-skimming mode, small non-uniformities in transfer threshold and detector capacitance do not cause non-uniformities in the video signal, making possible direct imaging without computer processing of the video signal. By using a surface-channel transfer gate between the Schottky diode and the buried-channel CCD structure, we can cut off (isolate) the Schottky diode from the BCCD output register and thus allow testing the CCD register at room temperature. The surface-channel transfer gate is also needed for the operation of the Schottky-diode detectors in the blooming control (saturation) mode (see Section IV-E).

IV. EXPERIMENTAL RESULTS

A. CCD Characteristics at 77 K

At room temperature the charge-transfer loss of the buried-channel CCD registers was typically 10^{-5} per transfer for operation with about 10% of bias charge and about 2×10^{-5} without the bias charge. At 77 K the transfer inefficiency was found to be larger, typically 5×10^{-5} with bias charge and 4×10^{-4} without bias charge.

For the infrared measurements reported here the line sensor and the output registers of the area sensor were always operated with a bias charge. However, the column registers of the area sensor have no provision for electrical input and thus exhibited some observable transfer inefficiency.

B. Dark (Leakage) Current of Platinum-Silicide Detectors

The theoretical dark current of an infrared-sensitive Schottky-barrier detector is due almost entirely to the internal thermionic emission of carriers from the metal over the barrier into the semiconductor. The current density for this process is given by [9]

$$J = A^{*}T^{2} \exp - \frac{q\psi_{ms}}{kT} \qquad (2)$$

where A^{*} is $\sim$ 32 A/cm^{2}K^2 for holes in Si, ψ_{ms} is the barrier height, q is the electronic charge, k is the Boltzmann's constant, and T is the detector temperature. For platinum-silicide Schottky-barrier detectors, the above dark-current density is 4×10^{-13} and 2×10^{-10} A/cm^2 for operation at temperatures of 77 and 90 K, respectively. In practice, the measured dark current of the platinum-silicide detectors tends to be increased by field concentration at the diode edges. This excess dark current can be controlled with n-type guard rings. Our experience shows that with the best devices operated at 80 K, no dark current is observed for thermal imaging with integration time in the range from 30 to 100 ms.

C. Infrared Test Set-Up

The experimental set-up used for infrared measurements consisted of an Electro-Optical Industries blackbody source and differential-temperature scene, Space Optics Research Lab IR optics, and an Air Products Displex refrigerator for cooling the arrays. The optics used included a four-element SORL f/1.2 Si/Ge lens which is AR coated for the 2-5 μm region.

For the infrared measurement, the sensors were cold-shielded and cold-filtered (3.4-4.2 μm) to minimize the background signal. The optical signals were imaged on the platinum-silicide sensor arrays through the back side of the optically-polished silicon substrate.

D. Uniformity

Because of low contrast in thermal scenes, spatial photoresponse non-uniformity can rapidly degrade the temperature sensitivity (NET) of staring arrays [17]. For example, a Schottky sensor with 4.5 μm cut-off has a signal-to-background contrast of 5%/K when responding to a 300 K scene. Therefore, a spatial uniformity of 0.5% is required to resolve 0.1 K [3]. As previously discussed, platinum-silicide Schottky-barrier IR-CCD's have inherently uniform response because photoyield is nearly independent of substrate doping concentration and lifetime. Thus it is possible to produce arrays which require no off-chip processing for individual pixel gain and no offset correction. The uniformity achieved with the 256-element IR-CCD line sensor is illustrated by the background response shown in Fig. 10. In Fig. 11 we show a typical portion of the line array illuminated by a 500 K blackbody source (through a 50% neutral density filter). The measured rms spatial non-uniformity across the line array is limited only by detector area variations due to the geometric definition of the diodes (i.e. reticulation).

E. Infrared Transfer Characteristics

The transfer characteristics of the 256-element IR-CCD sensor are shown in Fig. 12. The measured signal-to-noise ratio (S/N) is plotted versus the power density reaching the

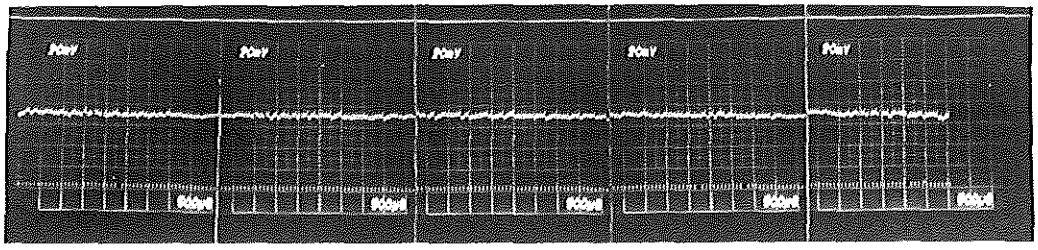

Fig. 10. Background response of 256-element IR-CCD line sensor with 3.4 to 4.2 μm band pass.

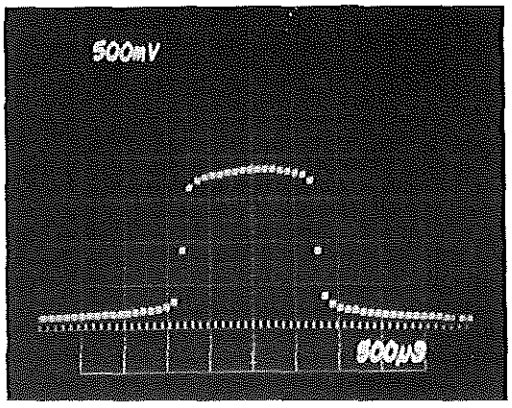

Fig. 11. Response of a typical portion of the 256-element IR-CCD line sensor as illuminated by a 500 K source (using 3.4 to 4.2 μm band pass filter and a 50% N.D. filter).

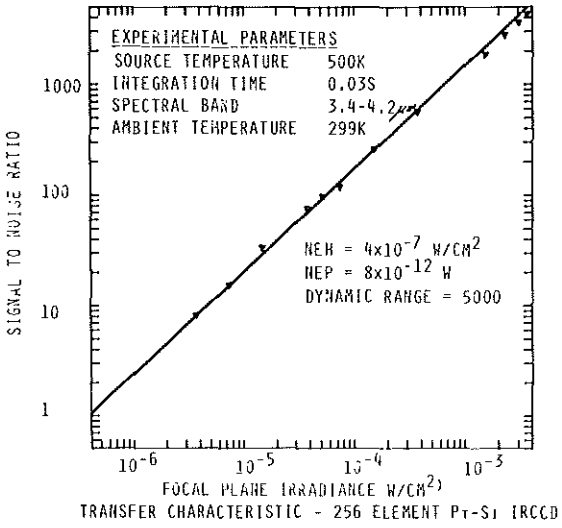

Fig. 12. Transfer characteristics of the 256-element IR-CCD line sensor.

back surface of the array. Since this array has no antireflective coatings, 30% of the incident power is reflected from the surface of the silicon substrate. The noise signal, determined by a superposition of the scope traces, corresponded to 2.0 mV peak-to-peak of which approximately 1.5 mV corresponds to a random noise and 1.5 mV to a coherent type of pick-up noise. From the curve in Fig. 12 we determine the noise-equivalent irradiance (NEH) in the 3.4-4.2 μm band as 4.5×10^{-7} W/cm^2 which corresponds to the noise-equivalent power (NEP) per pixel of 8×10^{-12} W. The measured dynamic range (S/N max) of the line sensor is 5,000. A similar measured transfer curve for the area sensor is shown in Fig. 13. In this case NEH = 1.8×10^{-6} W/cm^2, NEP = 3.4×10^{-11} W, and the dynamic range is 1,800.

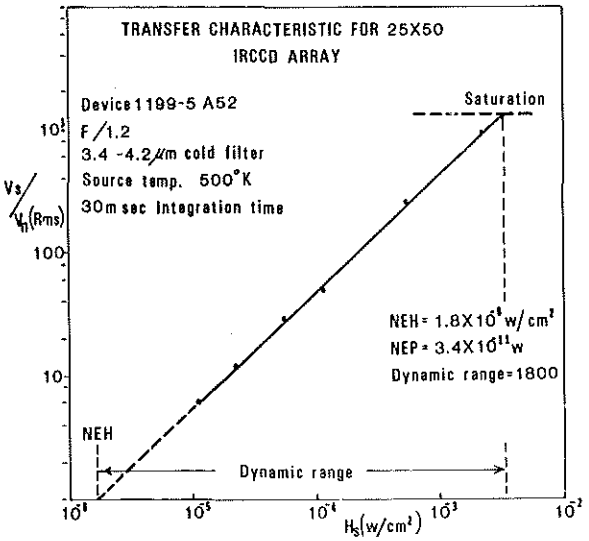

Fig. 13. Transfer characteristics of the 25x50-element IR-CCD area sensor.

Since the line sensor has been operated in the continuous-skimming mode, its dynamic range is limited by the capacity of the 50 μm-wide CCD output register. The area sensor is operated in the voltage-reset mode in which case the dynamic range of the sensor (the saturation level) is limited mainly by the effective capacitance of the detectors (estimated to be about 0.4 pF) and the amplitude of the transfer-gate voltage pulse, mentioned before in Section 3C. The Schottky-barrier detector design with a surface-channel transfer-gate and operated in the voltage-reset mode provides a built-in blooming-control mode of operation. In this mode the slope of the transfer curve past the saturation level (see Fig. 13) can be controlled by the duration of the transfer pulse.

The large dynamic range of the area sensor operating in the blooming control (saturation) mode is illustrated in Fig. 14. This figure shows a 10°C (above ambient) calibrated test grid detected by the area sensor with a match flame in the scene. While the match saturates the sensor where it is imaged, no blooming is observed. There is also no lag.

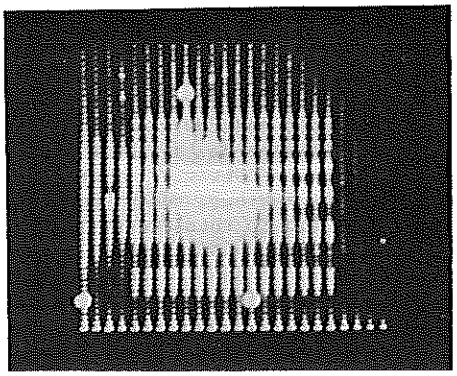

Fig. 14. A 10°C test grid and a match flame imaged by the 25x50-element IR-CCD area sensor.

F. Thermal Response

The thermal transfer response of the 256-element IR-CCD line sensor is shown in Fig. 15 for 30 ms integration time. The experimental points in this figure are compared to the calculated response obtained by integrating the product of the Schottky photoyield function and the Planck blackbody spectrum [2]. By using a differential blackbody target, the noise-equivalent temperature (NET) of this array for 30 ms stare time was measured as 0.8°C against a 24.0°C ambient. A more recently measured line array with 20 μm x 200 μm detectors exhibited a reduced NET of 0.4°C.

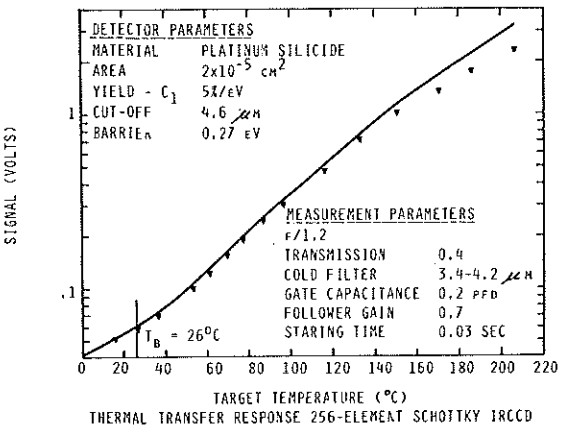

Fig. 15. Thermal response of the 256-element IR-CCD line sensor.

Fig. 16 shows the area-sensor image of radiation from a human hand (∿ 32°C in 26°C ambient). The weakest target observed with the 25x50 IR-CCD area sensor had temperatures slightly less than 1°C above ambient (26°C). The present measurements are limited by excess noise and low diode-breakdown voltages. Correcting the above problems should improve sensitivity by at least a factor of 5. Further, recent processing advances have led to thin diodes that are a factor of 2 more sensitive at all wavelengths. Thus we believe that both present devices could be improved so as to have NET in the range of 0.1 to 0.2°C.

Table I summarizes and compares parameters measured for both line and area sensors.

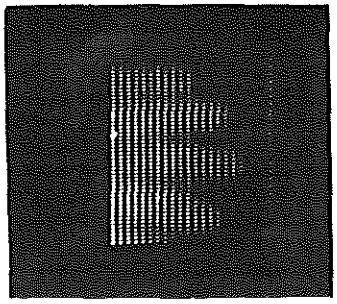

Fig. 16. 25x50-element IR-CCD camera image of human hand.

Table I

Parameters for 256-Element Linear and 25x50-Element Area PtSi IRCCD: 3.4-4.2 μm, 30 ms stare time

	Value		
Parameter	Line	Area	Comment
NET (°C)	0.8°C	1.0°C	0.4°C with larger area diodes ultimately 0.1°C.
NEH (W/cm^2)	$4.5x10^{-7}$	$1.8x10^{-6}$	
NEP (W)	$8x10^{-12}$	$3.36x10^{-11}$	
Linear Dynamic Range	5,000	1,800	Presently CCD limited for line array. Detector limited for area array.
Noise Level (mV p-p)	∿2 mV p-p	2 mV p-p	1.5 mV random; 1.5 mV coherent pick-up.
Photoresponse Uniformity (%)	0.55%	2%	Reticulation limited for line array.
Quantum Efficiency Coefficient (%/eV)	∿5%/eV	∿5%/eV	
Operating Temperature (K)	80 K	80 K	40 K-103 K
Transfer Inefficiency (per transfer)	$5x10^{-5}$	$5x10^{-5}$	77 K, 10% bias charge.

V. CONCLUSIONS

The advantages of the Schottky IR-CCD's are:

- high uniformity limited only by the geometric definition of the detectors
- high detector densities possible
- modest cooling requirements (in the range of 80 to 90 K)
- no optical cross-talk
- monolithic silicon construction with standard IC processing
- staring mode of operating
- no lag
- very large dynamic range
- antiblooming capability.

We have developed two types of IR-CCD's with Schottky-barrier platinum-silicide detectors, a 256-element line sensor and a 25x50-element area sensor.

We have demonstrated thermal imaging with a temperature discrimination of 1°C above ambient for the 25x50-element area sensor and 0.4°C for the 256-element line sensor.

With new designs and processing improvements, Schottky IR-CCD's with higher density and capable of temperature discrimination in the range of 0.1 to 0.2°C above ambient are anticipated. Such IR-CCD sensors, with resolution approaching that of commercial television, are expected to have applications in IR surveillance, reliability studies, and medical diagnostics.

REFERENCES

1. F. D. Shepherd,and A. C. Yang, "Silicon Schottky Retinas for Infrared Imaging," 1973 International Electron Devices Meeting, Technical Digest, pp. 310-313.

2. F. D. Shepherd, et al, "Silicon Schottky Barrier Monolithic IRTV Focal Planes," Advances in Electronics and Electron Physics, 40B, 981 (1975).

3. F. D. Shepherd, R. Taylor, S. Roosild, L. Skolnik, B. Cochrun, E. Kohn, "Ambient Thermal Response of Monolithic Schottky IRCCD's", Proceedings of IRIS Thermal Imaging Meeting, El Toro, CA, 1977.

4. E. Kohn, S. Roosild, F. Shepherd, and A. Yang, "Infrared Imaging with Monolithic, CCD-Addressed Schottky-Barrier Detector Arrays, Theoretical and Experimental Results," International Conference on Application of CCD's, 29-31 October 1975.

5. R. Taylor, F. Shepherd, S. Roosild, A. Yang, and E. Kohn, "Schottky IRCCD's," IRIS Detector Specialty Group Meeting, AF Academy, CO, March 1977.

6. L. Skolnik, R. Taylor, B. Capone, F. Shepherd, S. Roosild and W. F. Kosonocky, "A Platinum Silicide Schottky Barrier IR-CCD for Base Security Surveillance," 26th National IRIS, USAFA, Colorado Springs, 10 May 1978.

7. B. Capone, L. Skolnik, R. Taylor, F. Shepherd, S. Roosild, W. Ewing, W. Kosonocky, and E. Kohn, "Evaluation of a Schottky IRCCD Staring Mosaic Focal Plane," the 22nd International Technical Symposium of the Society of Photo-Optical Instrumentation Engineers, San Diego, Aug. 28-29, 1978.

8. W. F. Kosonocky, D. J. Sauer, and F. V. Shallcross, "256-Element Schottky-Barrier IRCCD Line Sensor," RADC-TR-77-304, September 1977.

9. E. S. Kohn, W. F. Kosonocky, and F. V. Shallcross, "Charge-Coupled Scanned IR Imaging Sensors," RADC-TR-77-303, September 1977.

10. W. F. Kosonocky, E. S. Kohn, and F. V. Shallcross, "Optimization Study of IR-CCD Array," RADC-TR-78, July 1978.

11. R. J. Archer and T. O. Yep, "Dependence of Schottky Barrier Height on Donor Concentration," J. Appl. Phys. 41, 303, 1970.

12. V. L. Dalal, "Analysis of Photoemissive Schottky-Barrier Photodetectors," J. Appl. Phys. 42, 2280 (1971).

13. V. E. Vickers, "Model of Schottky Barrier Hot-Electron-Mode Photodetection," Applied Optics, 10, 2190, 1971.

14. Wei-Kan Chu, S. S. Low, J. W. Mayer, M. Nicolet, "Analysis of Semiconductor Structures by Nuclear and Electrical Techniques, Silicide Formation," AFCRL-TR-75-0092, 31 January 1975.

15. C. L. Chen and J. T. Boyd, "Parallel Signal Injection in a CCD Using an Integrated Optical Channel Waveguide Array," IEEE T-ED, ED25, 2, 267-8, Feb. 1978.

16. J. M. White and S. G. Chamberlain, "A Multiple-Gate CCD-Photodiode Sensor Element for Imaging Arrays," IEEE T-ED, ED-25, pp 125-131, Feb. 1978.

17. J. A. Hall, "Problem of Infrared Television Camera Tubes vs Infrared Sensors," Applied Optics 10, p. 838, 1971.